

# Wnt/ $\beta$ -Catenin Participates in the Repair of Acute Respiratory Distress Syndrome-Associated Early Pulmonary Fibrosis via Mesenchymal Stem Cell Microvesicles

Xingcai Zhang<sup>1,\*</sup>, Lifang Ye<sup>2,\*</sup>, Wan Tang<sup>1</sup>, Yiqin Ji<sup>1</sup>, Li Zheng<sup>1</sup>, Yijun Chen<sup>1</sup>, Qidong Ge<sup>3</sup>, Changshun Huang<sup>1</sup>

<sup>1</sup>Department of Anesthesiology, Ningbo City First Hospital, Ningbo, Zhejiang, People's Republic of China; <sup>2</sup>Department of Anesthesiology, Zhujiang Hospital, Southern Medical University, Guangzhou, Guangdong, People's Republic of China; <sup>3</sup>Department of Breast Surgery, HuaMei Hospital, University of Chinese Academy of Sciences, Ningbo, Zhejiang, People's Republic of China

Correspondence: Changshun Huang; Qidong Ge, Tel +86-574-87085521, Fax +86-574-87085588, Email nbhcs1967@163.com; geqidong1986@126.com

\*These authors contributed equally to this work

**Purpose:** The main aim of the present study was to establish whether mesenchymal stem cell microvesicles (MSC MVs) exert anti-fibrotic effects and investigate the mechanisms underlying these effects in a mouse model of acute respiratory distress syndrome (ARDS)-associated early pulmonary fibrosis.

**Methods:** An ARDS-associated pulmonary fibrosis model was established in mice by an intratracheal injection of lipopolysaccharide (LPS). At 1, 3, and 7 days after LPS-mediated injury, the lungs of mice treated with MSC MVs and untreated controls were carefully excised and fibrosis was assessed based on the extent of collagen deposition. In addition, the development of epithelial-mesenchymal transition (EMT) was evaluated based on loss of E-cadherin and zona occludens-1 (ZO-1) along with the acquisition of  $\alpha$ -smooth muscle actin ( $\alpha$ -SMA) and N-cadherin. Nuclear translocation and  $\beta$ -catenin expression analyses were also used to evaluate activation of the Wnt/ $\beta$ -catenin signaling pathway.

**Results:** Blue-stained collagen fibers were evident as early as 7 days after LPS injection. Treatment with MSC MVs suppressed pathological progression to a significant extent. MSC MVs markedly reversed the upregulation of N-cadherin and  $\alpha$ -SMA and attenuated the downregulation of E-cadherin and ZO-1. The expression and nuclear translocation of  $\beta$ -catenin were clearly decreased on day 7 after MSC MV treatment.

**Conclusion:** Analyses indicated that MSC MVs could ameliorate ARDS-associated early pulmonary fibrosis via the suppression of EMT and might be related to Wnt/ $\beta$ -catenin transition signaling.

**Keywords:** mesenchymal stem cell, microvesicles, pulmonary fibrosis, ARDS, EMT, Wnt/ $\beta$ -catenin

## Introduction

Acute respiratory distress syndrome (ARDS) is an acute inflammatory pulmonary process triggered by severe pulmonary and systemic insults to the alveolar-capillary membrane. The pathophysiology of ARDS involves complex interactions among multiple mechanisms including immune cell infiltration, cytokine storms, alveolar-capillary barrier disruption, apoptosis, and the development of fibrosis. Abnormal tissue repair after lung injury leads to fibrotic changes, which are responsible for the high mortality rates of ARDS patients during the post-acute phase.<sup>1</sup> Several studies have shown that pulmonary fibrosis is an important contributory factor to poor prognosis of patients with acute lung injury (ALI) and fibrotic changes can occur in the early stages of ALI/ARDS.<sup>2</sup> The pathogenesis and pathological processes of pulmonary fibrosis involve four steps: injury to the lung tissue due to various causes, release of diverse pro-inflammatory and pro-fibrotic

mediators, destruction of tissue structures, and subsequent tissue repair.<sup>3</sup> Lung-protective mechanical ventilation (MV) along with other auxiliary approaches (prone position or judicious use of neuromuscular blocking agents) have been successfully used to reduce the mortality rates associated with this condition.<sup>4</sup> However, this approach can induce or aggravate lung damage, a condition referred to as mechanical ventilation-induced lung injury (VILI).<sup>5,6</sup> Adjuvant pharmacological approaches to reduce ARDS-associated pulmonary fibrosis have been highlighted as a potential means to improve morbidity and mortality rates. Over the past two decades, considerable research has focused on developing pharmacological therapies for ARDS, but results to date have been unsuccessful.<sup>7</sup>

Multiple preclinical studies have demonstrated the significant therapeutic potential of mesenchymal stem/stromal cells (MSC) for ALI despite a limited engraftment rate of 1–5%.<sup>8–10</sup> MSCs clearly have the capacity to suppress inflammation, reduce fibrosis, and prolong survival time in preclinical models of pulmonary fibrosis induced by bleomycin, silica, paraquat, and radiation.<sup>11–14</sup>

Bone marrow MSCs have been shown to attenuate silica-induced pulmonary fibrosis via the suppression of Wnt/ $\beta$ -catenin signaling.<sup>15</sup> However, MSCs have self-replicating capability with hazardous effects, including ectopic differentiation, tumor formation, genetic instability, and cellular rejection.<sup>16</sup> Recently, stem cell-derived treatments, such as MSC conditioned media (CM) and extracellular vesicles (EV), have generated considerable interest as potential “cell-free” options with similar therapeutic properties.<sup>17</sup> Previously, our group demonstrated that MSC microvesicles (MSC MVs) reduced lung inflammation, protein permeability, and pulmonary edema in endotoxin-induced ALI in mice.<sup>18</sup> However, to the best of our knowledge, whether MSC MVs have the ability to ameliorate LPS-induced ARDS-associated early pulmonary fibrosis has yet to be addressed. Similarly, nothing is known of the potential mechanisms that might be responsible for such effects.

The administration of human MSC-derived EVs (exosomes and microvesicles) on day 14 in a mouse model of bleomycin-induced pulmonary fibrosis led to significant downregulation of the mesenchymal marker,  $\alpha$ -smooth muscle actin ( $\alpha$ -SMA), and decreased histopathological fibrosis, thus indicating that the therapeutic effects of these vesicles on established lung fibrosis act by modifying the myofibroblastic phenotype.<sup>19</sup>

Epithelial–mesenchymal transition (EMT) has a significant impact on the pathogenesis of pulmonary fibrosis.<sup>20–22</sup> Coincidentally, recent studies have reported critical roles of Wnt/ $\beta$ -catenin signaling in epithelial cell proliferation, EMT, myofibroblast differentiation, and collagen synthesis.<sup>23,24</sup> Therefore, MSC MVs may present an effective therapeutic option to prevent the development of ARDS into pulmonary fibrosis. The present study was designed to determine the effects of MSC MVs on pulmonary fibrosis and changes in Wnt/ $\beta$ -catenin signaling pathway-related protein levels following exposure to LPS.

## Materials and Methods

### MSCs and the Isolation of MSC MVs

Mouse bone marrow-derived MSCs (MBMSC) were obtained from ScienCell Research Laboratories (Carlsbad, CA). These stem cells met all of the criteria for MSCs as defined by the International Society of Cellular Therapy.<sup>25</sup> MSCs were harvested from passage 8 were used for experimental use. MSC MVs were obtained from the supernatant fraction of MSCs as described previously.<sup>26,27</sup> Briefly, MSCs were cultured in MSC medium (MSC; Cat. No. 7501, ScienCell) with 5% fetal bovine serum (FBS, Cat. No. 0025), MSC growth supplement (MSCGS; Cat. No. 7552), and penicillin/streptomycin solution (P/S; Cat. No. 0503) until confluence in P150 flasks and subsequently serum-starved for 48 h in fresh conditioned medium (MSCM without FBS, MSCGS, and P/S). To isolate MVs, conditioned medium was centrifuged at 3000 rpm for 20 min to remove cellular debris, followed by centrifugation at 100,000 g (Beckman Coulter, Brea, CA, USA) for 1 h at 4°C. MSC MVs were washed in phosphate buffered saline (PBS) and subjected to a repeat ultracentrifugation step, resuspended according to the final MSC cell count after 48 h of serum starvation (10  $\mu$ L MVs per  $1 \times 10^6$  cells), and stored at  $-80^\circ\text{C}$  until further use (Figure 1).

### Identification of MSC MVs

The structure of the isolated MSC MVs was observed under a scanning electron microscope. MSC MVs were fixed with 3% (w/v) Karnovsky fixative for 2 h at  $48^\circ\text{C}$ . Monolayers were post-fixed for 2 h with 1% veronal buffered osmic acid

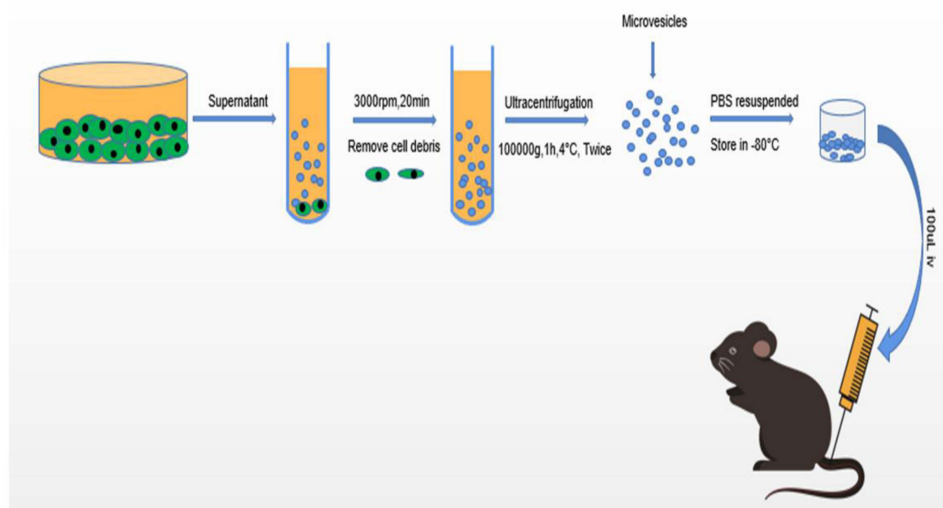


**Figure 1** Schematic diagram showing the isolation and identification of MSC MVs and animal experiment protocols.

and dehydrated in graded ethanols and/or propylene oxide. Cell preparations were then embedded in Epon or Araldite resin cured at 60°C. Thin sections were contrasted with saturated aqueous uranyl acetate and Reynolds lead citrate and subsequently imaged with a JEOL 1200 EX transmission electron microscope operating at 80 kV.<sup>28</sup> MVs were additionally assessed for diameter distribution by flow cytometry and subjected to Western blotting to identify specific markers, including CD63 and TSG101 (1:1000 dilution, Abcam, Cambridge, UK).

## Animal Experiments

The study protocol for animal experiments was approved by the Institutional Animal Care and Use Committee of Ningbo University (approval number 2019–189) and conformed to the guidelines of the National Institutes of Health Guidelines for the Care and Use of Laboratory Animals. Male C57BL/6 mice (8–10 weeks, ~ 25 g, n=70) were purchased from Charles River laboratories. Mice were housed under optimal pathogen-free laboratory conditions (25°C, 55% humidity and 12 h day/night cycle) and provided with a standard laboratory diet and water. After at least one week of acclimatization, mice were intraperitoneally anesthetized with chloral hydrate (4%) and administered with a single intratracheal dose of purified LPS (5 mg/kg) or PBS in a total volume of 50 µL.<sup>29</sup> LPS-treated mice were randomized into two groups that received either a vehicle or MSC MVs (100 µL) through the tail vein at 12 h after LPS-induced injury. The control and LPS groups received identical doses of normal saline. Lung samples from LPS-injured mice with or without MSC MV treatment were carefully excised and weighed on days 1, 3, and 7 after injury. The left lung was removed and fixed in 4% paraformaldehyde while the right lung was immediately stored at –80°C for further analysis.

## Histological Analysis of Lung Injury and Fibrosis

Left lung tissues were fixed in 4% paraformaldehyde and embedded in paraffin. After sequential staining with hematoxylin for 5 min and eosin for 2 min at 25°C and consecutive transverse slicing into 5 µm sections. The scoring criteria included pulmonary edema, bleeding, neutrophil infiltration and small airway injury, which was rated as 0–4 points according to the severity of the lesion: if no, <1/4, 1/4–1/2, 1/2–3/4, or ≥3/4 part of the area of microscopic field included the abnormal observations, the slide was scored as 0, 1, 2, 3, and 4, respectively. For each slide, three fields were examined to minimize regional variations. Lung fibrosis was evaluated by using staining tissues with Masson's trichrome, a stain that allows the identification of collagen. The degree of fibrosis was quantified based on the collagen content using Image J software.

## Western Blotting

Lung tissues were homogenized with lysis buffer containing protease and phosphatase inhibitors (50:1). The total protein concentration was measured using a BCA protein assay kit and 30 µg protein separated via 10% sodium dodecyl sulfate-

polyacrylamide gel electrophoresis (SDS-PAGE), followed by transfer to polyvinylidene fluoride membranes. After blocking in 5% bovine serum albumin (BSA) for 2 h, membranes were incubated overnight at 4°C with the following primary antibodies: E-cadherin (1:1000, Cell Signaling Technology, MA, USA), N-cadherin (1:1000, Cell Signaling Technology),  $\alpha$ -SMA (1:1000, Santa Cruz Biotechnology), ZO-1 (1:1000, Cell Signaling Technology),  $\beta$ -actin (1:2000, Santa Cruz Biotechnology), and  $\beta$ -catenin (1:2000, Cell Signaling Technology). The following morning, membranes were washed three times 10 min per wash and then incubated in Tris-buffered saline containing Tween 20 (TBST) supplemented with HRP-coupled anti-goat or anti-rabbit IgG antibodies (1:5000, Santa Cruz Biotechnology) for 1 h at room temperature. Protein bands were examined by fluorography with enhanced chemiluminescence (ECL) reagents and quantified with Image J and Bio-Rad software.

## Immunohistochemical Analysis

Paraffin-embedded lung sections were prepared, blocked with 3% H<sub>2</sub>O<sub>2</sub>, and incubated with primary antibodies against E-cadherin, N-cadherin,  $\alpha$ -SMA, ZO-1, and  $\beta$ -catenin (1:200) at 4°C overnight. Lung sections were washed, incubated with goat anti-rabbit secondary antibody (1:200) at room temperature for 1 h. The DAB-stained sections were postfixed in 1% OsO<sub>4</sub> for 30 min, reacted with 1% uranyl acetate for 20 min. The stained slides were imaged (x200) with a fluorescence microscope (Olympus Corporation, Tokyo, Japan).

## Statistical Analysis

Comparisons between two groups were carried out with the unpaired *t*-test. While, analysis of variance with Bonferroni correction was used to compare multiple groups. Values were considered statistically significant at *P* < 0.05. Statistical analyses were performed using ImageJ and GraphPad Prism software (San Diego, CA).

## Results

### Characterization of MSC MVs

MSC MVs were characterized by electron microscopy, Nanoparticle Tracking Analysis (NTA), and Western blotting. Scanning electron microscopy revealed that the isolation technique yielded a homogeneous population of spheroid particles (Figure 2A). NTA showed that the diameter of the MSC MVs approximately 67.72 nm (Figure 2C), with a concentration of  $1.16 \times 10^{11}$  particles per mL (Figure 2D). Western blotting analysis of the protein composition of MSC MVs showed that, the membrane protein, CD63, was abundantly expressed on exosomes; we also clearly detected the endosome-associated protein TSG101 (Figure 2B). These results confirmed that the MVs derived from MSCs exhibited the typical features of EVs in terms of size and the presence/distribution of protein markers.

### MSC MVs Suppressed LPS-Induced Lung Injury and Fibrosis

To establish a model of ARDS-associated early pulmonary fibrosis, we selected three different time-points (1, 3, and 7 days) after LPS instillation (Figure 3A and B). On day 7, a decrease in the inflammatory response was observed. Notably, pathological abnormalities were ameliorated by treatment with MSC MVs. Lung injury scores (Figure 3C) and the ratio of lung wet weight to body weight (LWW/BW; Figure 3D) were reduced at all time points following MSC MV treatment. Masson's staining revealed obvious collagen fibers on day 7 (stained blue) following LPS injection; only a limited number of collagen fibers were detected in lung tissues from mice in the MSC MV treatment groups (Figure 3E). Collectively, these findings clearly indicate that MSC MVs suppress the pathological progression of ARDS-associated early pulmonary fibrosis.

### MSC MVs Alleviated LPS-Induced EMT

Immunohistochemical analysis demonstrated a gradual reduction in the expression of E-cadherin and ZO-1 (Figure 4). Conversely, the expression of N-cadherin and  $\alpha$ -SMA gradually increased; the highest levels were detected on day 7 after LPS intervention (Figure 5). Notably, MSC MVs dramatically reversed the upregulation of N-cadherin and  $\alpha$ -SMA and attenuated the downregulation of E-cadherin and ZO-1 (Figures 4 and 5), suggesting that MSC MVs exert therapeutic effects on pulmonary fibrosis by inhibiting the EMT process.



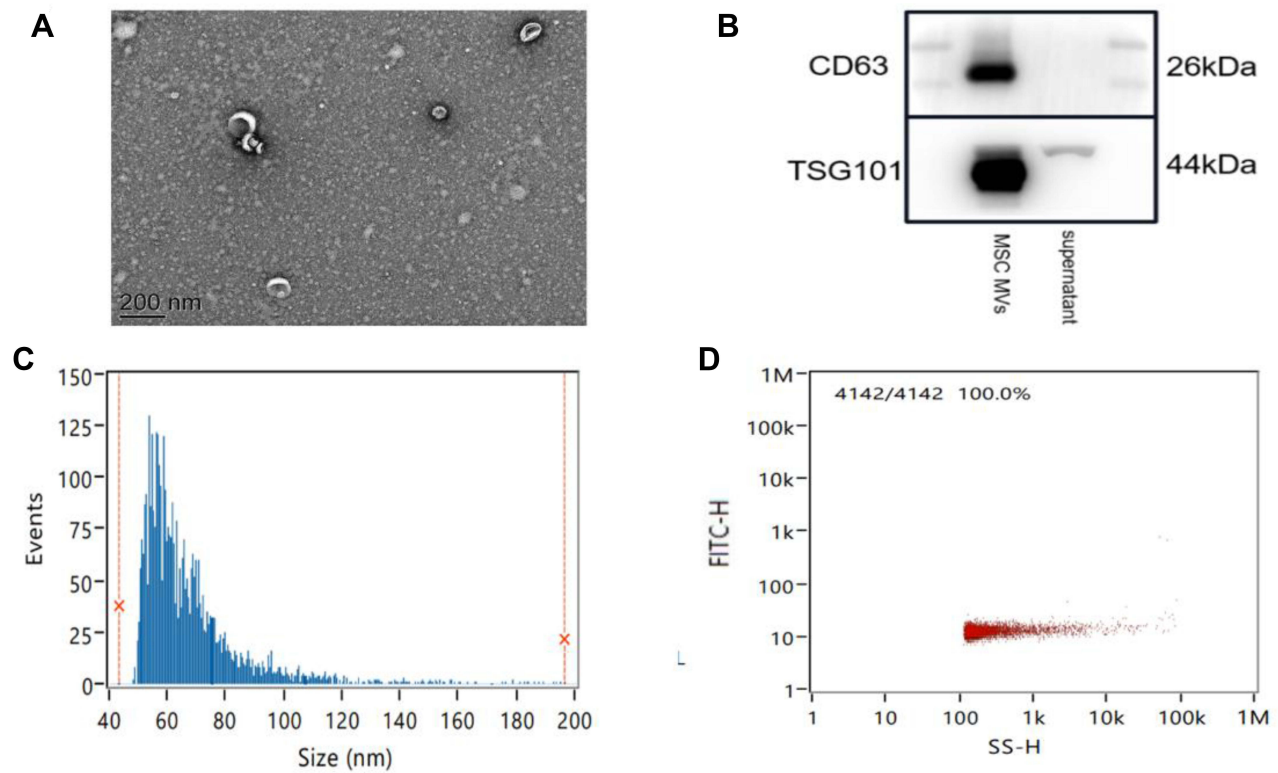


**Figure 2** The isolation and characterization of MSC MVs. **(A)** Transmission electron micrographs of MSC MVs. Scale bar, 200 nm. **(B)** Western blot analysis of MSC MV markers (CD63 and TSG101) in exosome preparations. **(C)** The size distribution profile of MSC MVs. **(D)** The concentration distribution profile of MSC MVs.

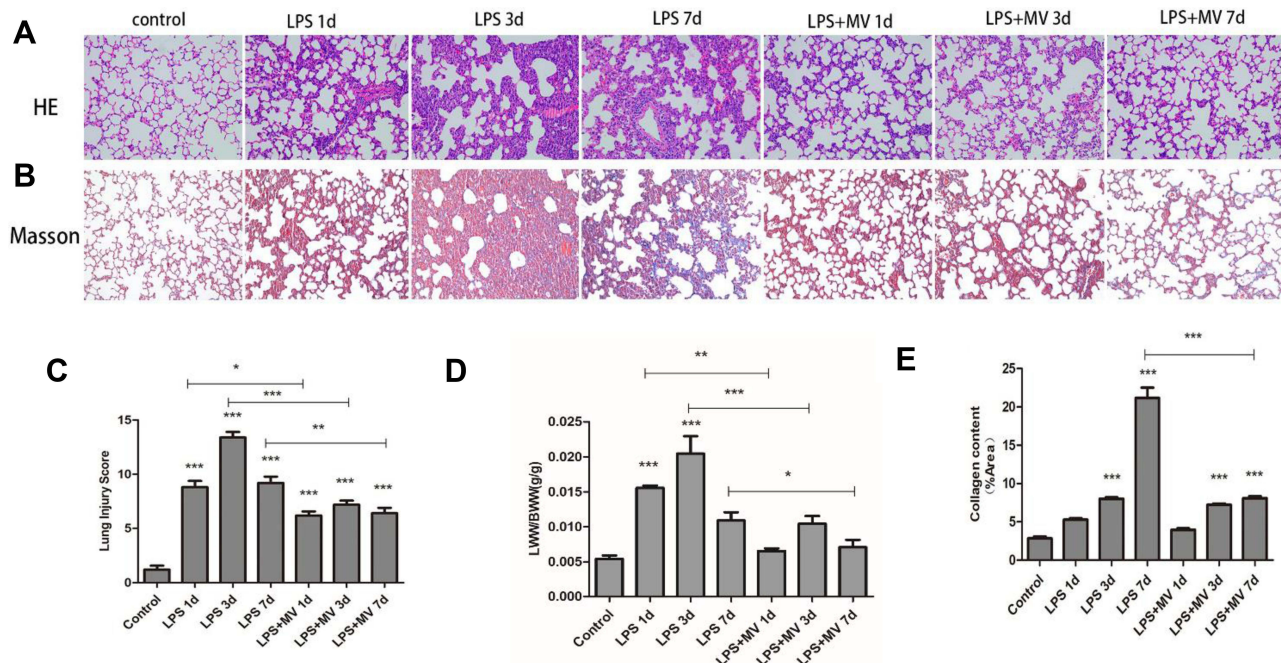


**Figure 3** Pathological changes in mouse lung tissue during development of ARDS. Representative images of lung tissues staining with HE **(A)** and Masson staining **(B)** in an animal model of ARDS (original magnification:  $\times 200$ ). Morphological alterations in lung sections were determined based on the lung injury score **(C)**. Lung permeability was assessed by measuring the LW/BW ratio **(D)**. Masson's trichrome staining was evaluated based on the area occupied by collagen **(E)**. Data are expressed as mean  $\pm$  SEM of at least three replicate experiments. \* $p < 0.05$ ; \*\* $p < 0.01$ ; \*\*\* $p < 0.001$  versus the control group.

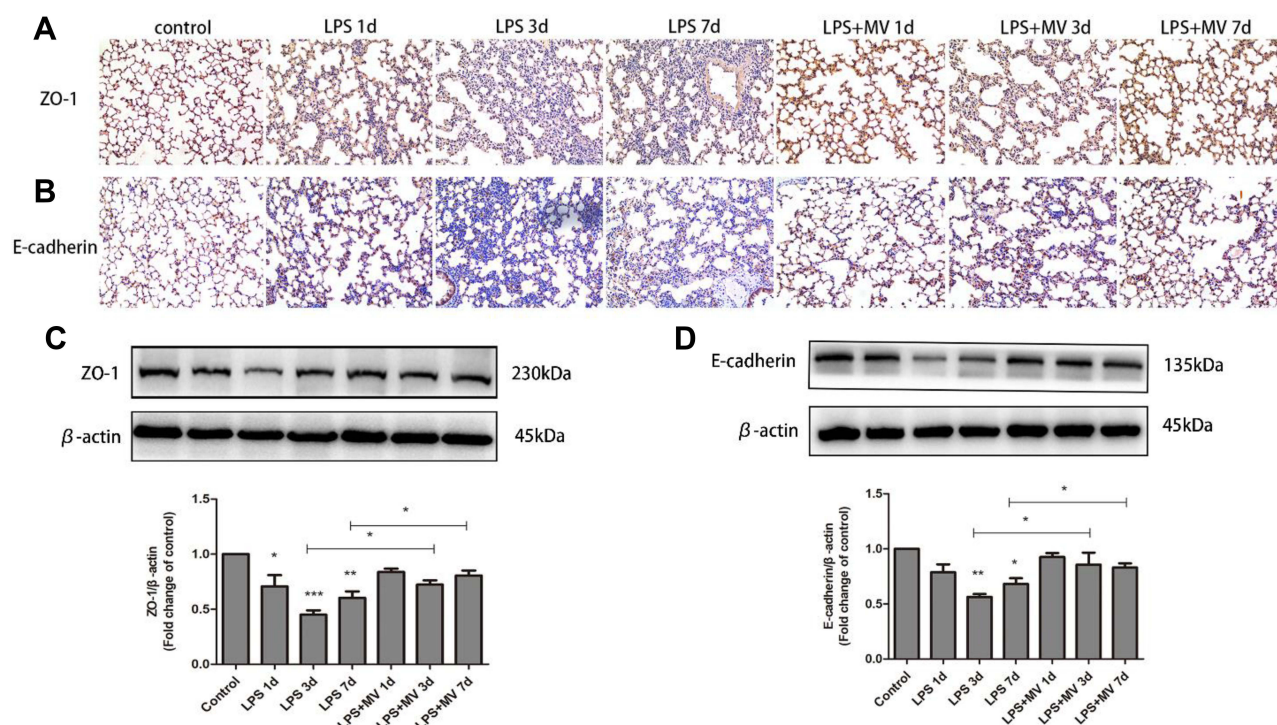


**Figure 4** MSC MVs protected the integrity of epithelial cells. Lung sections were subjected to immunohistochemical analysis using antibodies against ZO-1 (A) and E-cadherin (B); original magnification, x200. Western blot analysis was performed to determine the protein expression of ZO-1 (C) and E-cadherin (D). Data are expressed as means  $\pm$  SEM (n=6). \* $p$  <0.05; \*\* $p$  <0.01; \*\*\* $p$  <0.001 versus the control group.

## MSC MVs Inhibited the Wnt/ $\beta$ -Catenin Signaling

The nuclear translocation of  $\beta$ -catenin, signal that acts as a molecular switch in the Wnt pathway, was clearly observed on day 7 after LPS instillation (Figure 6A). Western blot experiments confirmed increased expression levels of  $\beta$ -catenin in the LPS model compared with the control group, particularly on day 7 (Figure 6B). Notably, after the transplantation of MSC MVs, the expression levels of  $\beta$ -catenin were significantly reduced when compared to the LPS model group. These findings suggest that MSC MVs exert an inhibitory effect on pulmonary fibrosis and may relate to suppressing the activation of the Wnt/ $\beta$ -catenin signaling pathway.

## Discussion

Pathologically, ARDS is characterized by an acute phase that involves bilateral pulmonary infiltration, severe hypoxemia, and pulmonary edema of non-cardiac origin; this is followed by a fibrotic phase in a large proportion of patients.<sup>30</sup> Previous studies reported that a single dose of intratracheal LPS injection could induce late pulmonary fibrosis from day 21 to 28 after administration.<sup>31</sup> However, Li et al<sup>32</sup> demonstrated that the repeated administration of LPS in rats for three consecutive days triggered rapid pulmonary fibrosis as early as 3–7 days after treatment. Early pulmonary fibrosis is an important contributory factor to a poor prognosis in patients with ARDS.<sup>2</sup> In view of these previous findings, we chose LPS to establish a model of ARDS. Then, we applied a specific time axis for experimentation such that we could capture the earliest point of evidence for fibrosis.

In the present study, an ARDS-associated pulmonary fibrosis mouse model was successfully replicated via the intratracheal injection of LPS. The lung injury and fibrosis scores of mice on day 7 following the injection of LPS were significantly higher than those of mice in the control group, thus providing clear evidence of LPS-induced lung injury and early pulmonary fibrosis.

Although numerous studies have explored the pathophysiological basis of ARDS, clinically available drugs have been unsuccessful in reducing the mortality, long-term mechanical ventilation, and length of ICU admission in patients with



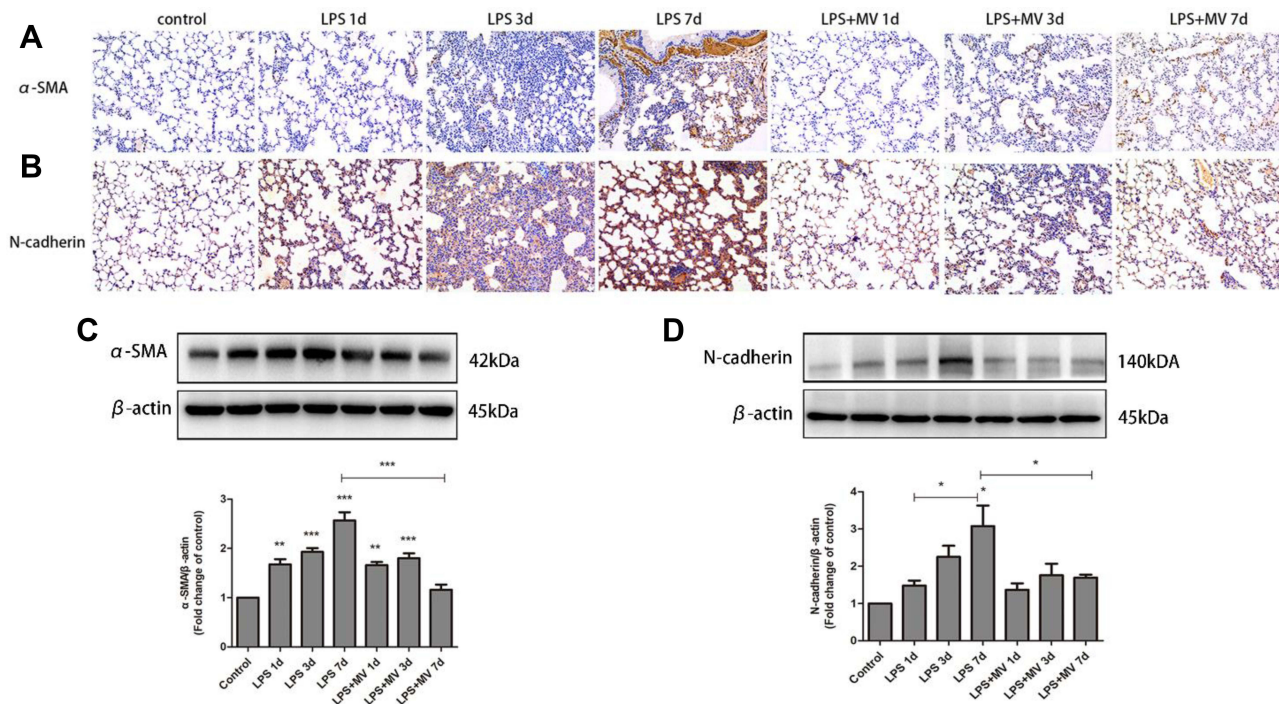


**Figure 5** MSC MVs attenuated the LPS-induced differentiation of myofibroblast. Lung sections were subjected to immunohistochemical analysis using antibodies against  $\alpha$ -SMA (**A**) and N-cadherin (**B**); original magnification,  $\times 200$ . Western blot analysis was performed to determine the protein expression levels of  $\alpha$ -SMA (**C**) and N-cadherin (**D**). Data are expressed as means  $\pm$  SEM ( $n=6$ ). \* $p < 0.05$ ; \*\* $p < 0.01$ ; \*\*\* $p < 0.001$  versus the control group.

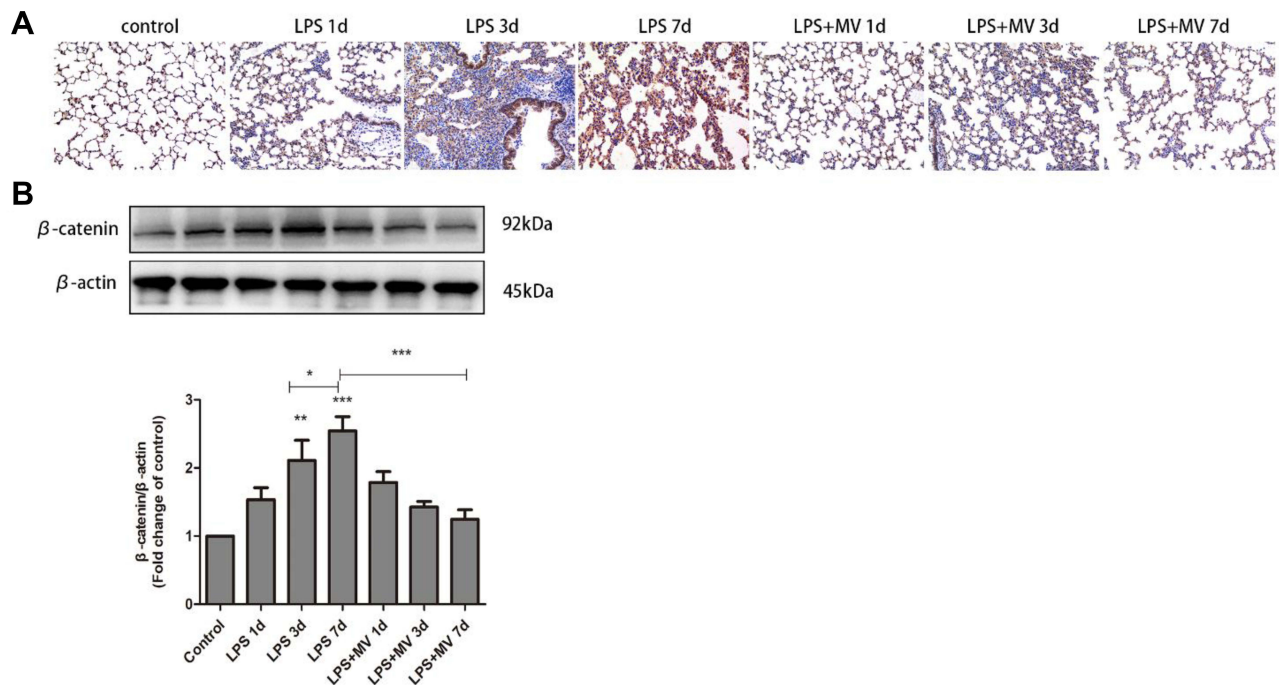


**Figure 6** MSC-MVs suppressed LPS-induced Wnt/ $\beta$ -catenin signaling. Immunohistochemical staining of  $\beta$ -catenin in mouse lung tissues (**A**). Western blot analysis of  $\beta$ -catenin levels (**B**). Data are expressed as means  $\pm$  SEM ( $n=6$ ). \* $p < 0.05$ ; \*\* $p < 0.01$ ; \*\*\* $p < 0.001$  versus the control group.

ARDS.<sup>33</sup> Despite the widespread adoption of ventilator strategies with low tidal volumes, investigators continue to report early fibroproliferative activity in the lungs of patients with ARDS.<sup>2</sup> Currently, the treatment options for ARDS remain limited. Previous authors have reported a high mortality rate of  $\sim 40\%$  in the United States; this clearly reflects the lack of

efficient medical countermeasures for ARDS.<sup>34,35</sup> Over the past few decades, MSCs, regarded as “the next pillar of medicine” have been shown to successfully reduce inflammatory response and collagen deposition,<sup>36</sup> reduce pulmonary vascular resistance, and improve vascular endothelial function and appropriate ventricular function in a bleomycin-induced model of lung injury.<sup>37,38</sup> Recent studies support the utility of MSC therapy as a potential option for treating cases of severe ARDS and cytokine storm resulting from the novel coronavirus disease COVID-19, although preclinical data are current lacking.<sup>39</sup> However, existing data suggests that only a small number of MSCs are capable of preferentially targeting damaged regions and surviving for over 24 h following systematic administration.<sup>40</sup> Moreover, due to poor quality control and inconsistent characteristics associated with immune compatibility, stability, heterogeneity, differentiation, and migration ability, substantial failures have been reported in many early and late-stage clinical trials.<sup>41,42</sup> As members of the MSC-derived secretome, MSC MVs and MSC EVs are known to exert a wealth of promising preclinical effects in lung diseases, such as bronchopulmonary dysplasia, acute ARDS, bronchial asthma, chronic obstructive pulmonary disease (COPD), idiopathic pulmonary fibrosis (IPF), pulmonary arterial hypertension, and silicosis.<sup>43</sup>

The intravenous administration of MSC MVs has been reported to significantly increase alveolar fluid rate clearance, reduce lung protein permeability, and reduce the levels of inflammation in injured alveoli following severe *E. coli* pneumonia in ex vivo perfused human lungs.<sup>17</sup> In a silica-induced mouse model of lung fibrosis, MVs derived from human BM-MSCs were effectively shown to reduce the recruitment of inflammatory cells into airways and reduce the deposition of collagen in the lung parenchyma.<sup>44</sup> However, to date, only limited research has focused on the mechanisms by which MSC MVs affect ARDS-associated early pulmonary fibrosis. Given that ARDS evolves in such a rapid manner, the optimal window for therapeutic intervention is most likely to be either preceding or coincident with the onset of fibroproliferation. In the present study, early intervention with MSC MVs was initiated prior to LPS-induced early pulmonary fibrosis. Notably, we observed a significant reduction of collagen deposition in the interstitium on day 7; moreover, lung tissue damage was markedly improved on days 3 and 7 after treatment with MSC MVs.

EMT, the process by which fully differentiated epithelial cells undergo mesenchymal phenotypic transformation to produce fibroblasts and myofibroblasts, is an important contributor to the development of fibrosis and is usually accompanied by changes in specific molecular markers.<sup>45</sup> Several studies have demonstrated that the transplantation of BMSCs can reduce pathological changes in the lungs of silica-treated animals, while also restoring epithelial characteristics, and reducing mesenchymal features (as demonstrated by the the expression profiles of specific proteins), thereby attenuating silica-induced pulmonary fibrosis in rats.<sup>14</sup> These previous experiments showed that MSC MVs restored the epithelial morphology of cells, at least to a certain extent. In our experiments, MSC MV treatment led to an inhibition in the LPS-induced expression of N-cadherin and  $\alpha$ -SMA while maintaining the levels of E-cadherin and ZO-1. These data collectively suggest that the MSC MV-mediated inhibition of LPS-induced EMT contributes to protective effects against LPS-induced pulmonary fibrosis.

The Wnt/ $\beta$ -catenin signaling pathway is known to play an important role in the pathological process of pulmonary fibrosis, thus suggesting that the suppression of this pathway could be used as a therapeutic strategy with which to alleviate pulmonary fibrosis.<sup>46,47</sup> Studies found that  $\beta$ -catenin expression was increased after LPS treatment and the therapeutic effects were mediated via interventions that reduce  $\beta$ -catenin expression, suggesting that  $\beta$ -catenin was a comparatively detrimental agent for cell survival.<sup>48–50</sup> In a previous study, Cheng and co-workers reported that the activation of  $\beta$ -catenin promotes LPS-induced ALI.<sup>51</sup> Similarly, Jang et al reported that  $\beta$ -catenin was involved in the inflammatory responses of LPS-stimulated BEAS-2B human bronchial epithelial cells.<sup>52</sup> Villar et al<sup>53</sup> confirmed abnormal activation of Wnt/ $\beta$ -catenin in patients with early sepsis-related ARDS that was associated with lung inflammation and profibrosis. The nuclear translocation of  $\beta$ -catenin, a process that acts as a molecular switch in the Wnt pathway, is known to represent a hallmark of Wnt/ $\beta$ -catenin activation.<sup>54</sup> Data from this study showed high expression levels of  $\beta$ -catenin in the lung tissue on day 7 after the intratracheal injection of LPS, which was suppressed in the MSC MV treatment groups. Furthermore, the nuclear translocation of  $\beta$ -catenin was observed on day 7 in mice treated with LPS.

Our study has some limitations that should be considered. First, our investigations of the role of MSC MVs in pulmonary disease and development were based on an animal model; it is not clear how these findings can be translated



to human medicine. Second, while a single dose of MVs clearly induced therapeutic effects, we should also consider the application of multiple doses, as this approach has consistently been associated with superior outcomes. Third, we did not acquire evidence for the alleviation of lung injury and fibrogenesis following the knockout or pharmacological inhibition of  $\beta$ -catenin. This suggests that the Wnt/ $\beta$ -catenin signaling only participates in pulmonary fibrosis.

## Conclusion

In summary, MVs released from MSCs exerted protective effects on early fibrosis by suppressing EMT in LPS-induced ARDS. The mechanism underlying the therapeutic activity of MSC MVs potentially may involve the inhibition of the Wnt/ $\beta$ -catenin signaling pathway.

## Acknowledgments

This research was supported by the Medical and Health Plan of Zhejiang (grant number: 2019KY581) and the National Science Foundation of Ning Bo (grant number: 202003N4272). We are grateful to the Central Laboratory of Ningbo First Hospital.

## Disclosure

The authors have no conflicts of interest to declare.

## References

1. Villar J, Zhang H, Slutsky AS. Lung repair and regeneration in ARDS: role of PECAM1 and Wnt signaling. *Chest*. 2019;155:587–594. doi:10.1016/j.chest.2018.10.022
2. Burnham EL, Janssen WJ, Riches DW, et al. The fibroproliferative response in acute respiratory distress syndrome: mechanisms and clinical significance. *Eur Respir J*. 2014;43:276–285. doi:10.1183/09031936.00196412
3. Ding Q, Luckhardt T, Hecker L, et al. New insights into the pathogenesis and treatment of idiopathic pulmonary fibrosis. *Drugs*. 2011;71:981–1001. doi:10.2165/11591490-000000000-00000
4. Beitler JR, Malhotra A, Thompson BT. Ventilator-induced lung injury. *Clin Chest Med*. 2016;37:633–646. doi:10.1016/j.ccm.2016.07.004
5. Wang Y, Minshall RD, Schwartz DE, et al. Cyclic stretch induces alveolar epithelial barrier dysfunction via calpain-mediated degradation of p120-catenin. *Am J Physiol Lung Cell Mol Physiol*. 2011;301:L197–L206. doi:10.1152/ajplung.00048.2011
6. Ju H, Li Y, Xing X, et al. Manganese-12 acetate suppresses the migration, invasion, and epithelial-mesenchymal transition by inhibiting Wnt/ $\beta$ -catenin and PI3K/AKT signaling pathways in breast cancer cells. *Thorac Cancer*. 2018;9:353–359. doi:10.1111/1759-7714.12584
7. Wang X, Lai R, Su X, et al. Edaravone attenuates lipopolysaccharide-induced acute respiratory distress syndrome associated early pulmonary fibrosis via amelioration of oxidative stress and transforming growth factor- $\beta$ /Smad3 signaling. *Biochem Biophys Res Commun*. 2018;495:706–712. doi:10.1016/j.bbrc.2017.10.165
8. Kotton DN, Fabian AJ, Mulligan RC. Failure of bone marrow to reconstitute lung epithelium. *Am J Respir Cell Mol Biol*. 2005;33:328–334. doi:10.1165/rcmb.2005-0175RC
9. Loi R, Beckett T, Goncz KK, et al. Limited restoration of cystic fibrosis lung epithelium in vivo with adult bone marrow-derived cells. *Am J Respir Crit Care Med*. 2006;173:171–179. doi:10.1164/rccm.200502-309OC
10. Pittenger MF, Mackay AM, Beck SC, et al. Multilineage potential of adult human mesenchymal stem cells. *Science*. 1999;284:143–147. doi:10.1126/science.284.5411.143
11. Chen J, Si L, Zhou L, et al. Role of bone marrow mesenchymal stem cells in the development of PQ-induced pulmonary fibrosis. *Mol Med Rep*. 2019;19:3283–3290. doi:10.3892/mmr.2019.9976
12. He F, Wang Y, Li Y, et al. Human amniotic mesenchymal stem cells alleviate paraquat-induced pulmonary fibrosis in rats by inhibiting the inflammatory response. *Life Sci*. 2020;243:117290. doi:10.1016/j.lfs.2020.117290
13. Periera-Simon S, Xia X. Anti-fibrotic effects of different sources of MSC in bleomycin-induced lung fibrosis in C57BL6 male mice. *Respirology*. 2021;26:161–170. doi:10.1111/resp.13928
14. Zhang E, Yang Y, Chen S, et al. Bone marrow mesenchymal stromal cells attenuate silica-induced pulmonary fibrosis potentially by attenuating Wnt/ $\beta$ -catenin signaling in rats. *Stem Cell Res Ther*. 2018;9:311. doi:10.1186/s13287-018-1045-4
15. Tieu A, Lalu MM. An analysis of mesenchymal stem cell-derived extracellular vesicles for preclinical use. *ACS Nano*. 2020;14:9728–9743. doi:10.1021/acsnano.0c01363
16. Jafarinia M, Alsahebhosoul F. Mesenchymal stem cell-derived extracellular vesicles: a novel cell-free therapy. *Immunol Invest*. 2020;49:758–780. doi:10.1080/08820139.2020.1712416
17. Park J, Kim S, Lim H, et al. Therapeutic effects of human mesenchymal stem cell microvesicles in an ex vivo perfused human lung injured with severe E. coli pneumonia. *Thorax*. 2019;74:43–50. doi:10.1136/thoraxjnl-2018-211576
18. Hu S, Park J, Liu A, et al. Mesenchymal stem cell microvesicles restore protein permeability across primary cultures of injured human lung microvascular endothelial cells. *Stem Cell Transl Med*. 2018;7:615–624. doi:10.1002/sctm.17-0278
19. Shentu TP, Huang TS, Cernelc-Kohan M, et al. Thy-1 dependent uptake of mesenchymal stem cell-derived extracellular vesicles blocks myofibroblastic differentiation. *Sci Rep*. 2017;7:18052. doi:10.1038/s41598-017-18288-9

20. Han YY, Shen P, Chang WX. Involvement of epithelial-to-mesenchymal transition and associated transforming growth factor- $\beta$ /Smad signaling in paraquat-induced pulmonary fibrosis. *Mol Med Rep*. 2015;12:7979–7984. doi:10.3892/mmr.2015.4454
21. Jolly MK, Ward C, Eapen MS. Epithelial-mesenchymal transition, a spectrum of states: role in lung development, homeostasis, and disease. *Dev Dyn*. 2018;247:346–358. doi:10.1002/dvdy.24541
22. Yamada A, Aki T, Unuma K, et al. Paraquat induces epithelial-mesenchymal transition-like cellular response resulting in fibrogenesis and the prevention of apoptosis in human pulmonary epithelial cells. *PLoS One*. 2015;10:e0120192. doi:10.1371/journal.pone.0120192
23. Burgy O, Königshoff M. The WNT signaling pathways in wound healing and fibrosis. *Matrix Biol*. 2018;68–69:67–80. doi:10.1016/j.matbio.2018.03.017
24. Chen X, Shi C, Cao H, et al. The hedgehog and Wnt/ $\beta$ -catenin system machinery mediate myofibroblast differentiation of LR-MSCs in pulmonary fibrogenesis. *Cell Death Dis*. 2018;9:639. doi:10.1038/s41419-018-0692-9
25. Dominici M, Le Blanc K, Mueller I, et al. Minimal criteria for defining multipotent mesenchymal stromal cells. The International Society for Cellular Therapy position statement. *Cytotherapy*. 2006;8:315–317. doi:10.1080/14653240600855905
26. Zhu YG, Feng XM, Abbott J, et al. Human mesenchymal stem cell microvesicles for treatment of Escherichia coli endotoxin-induced acute lung injury in mice. *Stem Cells*. 2014;32:116–125. doi:10.1002/stem.1504
27. Bruno S, Grange C, Collino F, et al. Microvesicles derived from mesenchymal stem cells enhance survival in a lethal model of acute kidney injury. *PLoS One*. 2012;7:e33115. doi:10.1371/journal.pone.0033115
28. Tang XD, Shi L, Monsel A, et al. Mesenchymal stem cell microvesicles attenuate acute lung injury in mice partly mediated by Ang-1 mRNA. *Stem Cells*. 2017;35:1849–1859. doi:10.1002/stem.2619
29. Wei W, Bing M, Heng-yu L, et al. Biphasic effects of selective inhibition of transforming growth factor  $\beta$ 1 activin receptor-like kinase on LPS-induced lung injury. *Shock*. 2010;33:218–224. doi:10.1097/shk.0b013e3181ae7f36
30. Yang Y, Hu L, Xia H, et al. Resolvin D1 attenuates mechanical stretch-induced pulmonary fibrosis via epithelial-mesenchymal transition. *Am J Physiol Lung Cell Mol Physiol*. 2019;316:L1013–L1024. doi:10.1152/ajplung.00415.2018
31. Zhang YQ, Liu YJ, Mao YF, et al. Resveratrol ameliorates lipopolysaccharide-induced epithelial mesenchymal transition and pulmonary fibrosis through suppression of oxidative stress and transforming growth factor- $\beta$ 1 signaling. *Clin Nutr*. 2015;34:752–760. doi:10.1016/j.clnu.2014.08.014
32. Li H, Du S, Yang L, et al. Rapid pulmonary fibrosis induced by acute lung injury via a lipopolysaccharide three-hit regimen. *Innate Immun*. 2009;15:143–154. doi:10.1177/1753425908101509
33. Bosma KJ, Taneja R, Lewis JF. Pharmacotherapy for prevention and treatment of acute respiratory distress syndrome: current and experimental approaches. *Drugs*. 2010;70:1255–1282. doi:10.2165/10898570-000000000-00000
34. Máca J, Jor O, Holub M, et al. Past and present ARDS mortality rates: a systematic review. *Respir Care*. 2017;62:113–122. doi:10.4187/respcare.04716
35. Maybauer MO, Maybauer DM, Herndon DN. Incidence and outcomes of acute lung injury. *N Engl J Med*. 2006;354:416–7; author reply 416–7.
36. Moodley Y, Atienza D, Manuelpillai U, et al. Human umbilical cord mesenchymal stem cells reduce fibrosis of bleomycin-induced lung injury. *Am J Pathol*. 2009;175:303–313. doi:10.2353/ajpath.2009.080629
37. Schmuck EG, Hacker TA, Schreier DA, et al. Beneficial effects of mesenchymal stem cell delivery via a novel cardiac bioscaffold on right ventricles of pulmonary arterial hypertensive rats. *Am J Physiol Heart Circ Physiol*. 2019;316:H1005–H1013. doi:10.1152/ajpheart.00091.2018
38. Badr Eslam R, Croce K, Mangione FM, et al. Persistence and proliferation of human mesenchymal stromal cells in the right ventricular myocardium after intracoronary injection in a large animal model of pulmonary hypertension. *Cytotherapy*. 2017;19:668–679. doi:10.1016/j.jcyt.2017.03.002
39. Yen BL, Yen ML, Wang LT, et al. Current status of mesenchymal stem cell therapy for immune/inflammatory lung disorders: gleanings insights for possible use in COVID-19. *Stem Cells Transl Med*. 2020;9:1163–1173. doi:10.1002/sctm.20-0186
40. Schrepfer S, Deuse T, Reichenspurner H, et al. Stem cell transplantation: the lung barrier. *Transplant Proc*. 2007;39:573–576. doi:10.1016/j.transproceed.2006.12.019
41. Conrad C, Niess H, Huss R, et al. Multipotent mesenchymal stem cells acquire a lymphendothelial phenotype and enhance lymphatic regeneration in vivo. *Circulation*. 2009;119:281–289. doi:10.1161/circulationaha.108.793208
42. Haga H, Yan IK, Takahashi K, et al. Tumour cell-derived extracellular vesicles interact with mesenchymal stem cells to modulate the microenvironment and enhance cholangiocarcinoma growth. *J Extracell Vesicles*. 2015;4:24900. doi:10.3402/jev.v4.24900
43. Guo H, Su Y. Effects of mesenchymal stromal cell-derived extracellular vesicles in lung diseases: current status and future perspectives. *Stem Cell Rev Rep*. 2021;17:440–458. doi:10.1007/s12015-020-10085-8
44. Choi M, Ban T, Rhim T. Therapeutic use of stem cell transplantation for cell replacement or cytoprotective effect of microvesicle released from mesenchymal stem cell. *Mol Cells*. 2014;37:133–139. doi:10.14348/molcells.2014.2317
45. Kalluri R, Neilson EG. Epithelial-mesenchymal transition and its implications for fibrosis. *J Clin Invest*. 2003;112:1776–1784. doi:10.1172/jci20530
46. Wang C, Zhu H, Sun Z, et al. Inhibition of Wnt/ $\beta$ -catenin signaling promotes epithelial differentiation of mesenchymal stem cells and repairs bleomycin-induced lung injury. *Am J Physiol Cell Physiol*. 2014;307:C234–C244. doi:10.1152/ajpcell.00366.2013
47. Wang X, Dai W, Wang Y, et al. Blocking the Wnt/ $\beta$ -catenin pathway by lentivirus-mediated short hairpin RNA targeting  $\beta$ -catenin gene suppresses silica-induced lung fibrosis in mice. *Int J Environ Res Public Health*. 2015;12:10739–10754. doi:10.3390/ijerph120910739
48. Monick MM, Carter AB, Robeff PK, et al. Lipopolysaccharide activates Akt in human alveolar macrophages resulting in nuclear accumulation and transcriptional activity of beta-catenin. *J Immunol*. 2001;166:4713–4720. doi:10.4049/jimmunol.166.7.4713
49. Lee H, Bae S, Choi BW, et al. WNT/ $\beta$ -catenin pathway is modulated in asthma patients and LPS-stimulated RAW264.7 macrophage cell line. *Immunopharmacol Immunotoxicol*. 2012;34:56–65. doi:10.3109/08923973.2011.574704
50. Gong K, Zhou F, Huang H, et al. Suppression of GSK3 $\beta$  by ERK mediates lipopolysaccharide induced cell migration in macrophage through  $\beta$ -catenin signaling. *Protein Cell*. 2012;3:762–768. doi:10.1007/s12328-012-2058-x
51. Cheng L, Zhao Y, Qi D, et al. Wnt/ $\beta$ -catenin pathway promotes acute lung injury induced by LPS through driving the Th17 response in mice. *Biochem Biophys Res Commun*. 2018;495:1890–1895. doi:10.1016/j.bbrc.2017.12.058

52. Jang J, Ha JH, Chung SI, et al. B-catenin regulates NF- $\kappa$ B activity and inflammatory cytokine expression in bronchial epithelial cells treated with lipopolysaccharide. *Int J Mol Med*. 2014;34:632–638. doi:10.3892/ijmm.2014.1807
53. Villar J, Cabrera-Benítez NE, Ramos-Nuez A, et al. Early activation of pro-fibrotic WNT5A in sepsis-induced acute lung injury. *Crit Care*. 2014;18:568. doi:10.1186/s13054-014-0568-z
54. Chilosi M, Poletti V, Zamò A, et al. Aberrant Wnt/ $\beta$ -catenin pathway activation in idiopathic pulmonary fibrosis. *Am J Pathol*. 2003;162:1495–1502. doi:10.1016/s0002-9440(10)64282-4

## Drug Design, Development and Therapy

Dovepress

### Publish your work in this journal

Drug Design, Development and Therapy is an international, peer-reviewed open-access journal that spans the spectrum of drug design and development through to clinical applications. Clinical outcomes, patient safety, and programs for the development and effective, safe, and sustained use of medicines are a feature of the journal, which has also been accepted for indexing on PubMed Central. The manuscript management system is completely online and includes a very quick and fair peer-review system, which is all easy to use. Visit <http://www.dovepress.com/testimonials.php> to read real quotes from published authors.

Submit your manuscript here: <https://www.dovepress.com/drug-design-development-and-therapy-journal>